Repurposing Quetiapine as an Adjuvant Therapeutic Agent for Triple-Negative Breast Cancer

[1]Ling He*, [1]Purva Joshi, [1]Angeliki Ioannidis, [1]Anoushka Kathiravan, [1]Mohammad Saki, [1,2,3]Frank Pajonk

[1]Department of Radiation Oncology, David Geffen School of Medicine at UCLA

[2]Department of Neurosurgery, David Geffen School of Medicine at UCLA

[3]Jonsson Comprehensive Cancer Center at UCLA

***Correspondence address:** Ling He, PhD, Department of Radiation Oncology, David Geffen School of Medicine at UCLA, 10833 Le Conte Ave, Los Angeles, CA 90095-1714, Phone: +1 310 206 8733, Fax: +1 310 206 1260, email: LingHe@mednet.ucla.edu

Abstract

Background: The lack of a molecular target in triple-negative breast cancer (TNBC) makes it one of the most challenging breast cancers to treat. Current standard-of-care primarily relies on cytotoxic chemotherapy and radiotherapy, but long-term outcomes remain poor largely due to early relapse, therapy resistance, and high incidents of metastases. More recently, dopamine signaling has emerged as a novel area of interest in cancer biology. Dopamine receptors have been implicated in tumor progression, maintenance of cancer stem-like cells, and therapy resistance in various malignancies, including TNBC. Quetiapine (QTP), an FDA-approved atypical antipsychotic and DRD2/DRD3 antagonist, has shown preclinical efficacy in glioblastoma. However, its anti-tumor potential in TNBC remains unexplored.

Methods: Clonogenic survival and mammosphere-forming assays were used to evaluate QTP's anti-tumor activity in TNBC cell lines (SUM159-PT, BT-549, and MDA-MB-231). Cells were treated with QTP alone or in combination with a single dose of 4 Gy radiation or standard chemotherapeutic agents (doxorubicin, paclitaxel, 5-fluorouracil). Apoptotic cell death was evaluated using Annexin V/propidium iodide flow cytometry, while DNA double-strand breaks were assessed through γ-H2AX staining. Transwell assays were conducted to examine QTP's impact on both untreated bulk tumor cells and those surviving sublethal radiation exposure. Additionally, the effect of QTP on DNA repair dynamics was investigated by monitoring the resolution of γ-H2AX foci over time following treatment.

Results: QTP significantly reduced clonogenicity and self-renewal in all TNBC models tested, both alone and in combination with radiation or chemotherapy. In apoptosis

assays, QTP treatment induced a marked increase in early and late apoptotic cell populations. QTP also promoted DNA double-strand break formation and delayed repair, as indicated by persistent γ-H2AX foci at 24 hours post-treatment. Additionally, QTP impaired the migratory capacity of both untreated and radiation-surviving cells. Combination treatments with QTP and doxorubicin produced synergistic effects, resulting in complete loss of colony-forming ability and mammosphere formation.

Conclusions: The data presented in this study support the repurposing of quetiapine as an adjuvant therapeutic agent alongside radiotherapy and chemotherapy in TNBC. By targeting apoptosis, DNA repair, and cancer cell migration, QTP offers a novel, multi-faceted approach to improving outcomes in this high-risk breast cancer subtype.

Keywords

Triple-negative breast cancer, quetiapine, dopamine receptor, cancer stem cell, radiation therapy, chemotherapy

Introduction

Breast cancer remains the most commonly diagnosed cancer among women, accounting for approximately 30 % (or 1 in 3) of all new female cancer cases each year. Among these, triple-negative breast cancer (TNBC) constitutes an estimated 10 – 15 % of all cases, which translates to roughly 30,000 to 45,000 new diagnoses annually in the United States (1, 2) (https://www.nationalbreastcancer.org/breast-cancer-facts/). TNBC is defined by a lack of estrogen receptor (ER), progesterone receptor (PR), and human epidermal growth factor receptor 2 (HER2), that are commonly used as therapeutic targets in other breast cancer subtypes. Due to this absence of targetable biomarkers, TNBC has been recognized as one of the most aggressive and therapeutically challenging forms of breast cancer (3-5).

Despite continued advances in early detection and prevention strategies, the American Cancer Society predicts that the number of newly diagnosed invasive breast cancer cases is expected to rise further in 2025 (https://www.cancer.org/cancer/types/breast-cancer/about/how-common-is-breast-cancer.html), highlighting the persistent burden of the disease. TNBC is associated with rapid tumor progression, increased rates of distant metastasis, early relapse -often within the first three years of diagnosis- and significantly worse overall survival compared to other forms of breast cancer (6, 7). The current standard-of-care relies heavily on cytotoxic chemotherapy and radiotherapy, as targeted hormonal and HER2-directed therapies are ineffective in this case (8, 9). However, the clinical benefit of chemotherapy and/or radiotherapy is often limited by TNBC's pronounced intra-tumoral heterogeneity, high proliferative rate, and frequent enrichment

77 of therapy-resistant cancer stem-like cells, which attribute to treatment failure and
78 recurrence (10, 11). Collectively, these challenges underscore an urgent and unmet need
79 for the development of novel therapeutic strategies that can effectively overcome
80 treatment resistance, eradicate tumor-initiating cells, and ultimately improve long-term
81 outcomes for patients with this aggressive disease subtype.

82

83 Dopamine is a well-characterized neurotransmitter that plays a central role in regulating
84 numerous complex brain functions, including mood, motivation, cognition, and motor
85 control (12, 13). Interestingly, beyond its neurological roles, emerging evidence has
86 highlighted dopamine signaling as a potential modulator in cancer biology (14-18). In
87 particular, the D2-like class of dopamine receptors -which includes DRD2, DRD3, and
88 DRD4- has been found to be upregulated in various malignancies and linked to cancer
89 cell stemness (19-21). Moreover, reduced cancer risk has been correlated with disorders
90 such as schizophrenia and Parkinson's disease (19, 22), in which dopaminergic drugs
91 are used, suggesting a potential protective role of dopamine receptor antagonism in
92 cancer development.

93

94 Quetiapine (QTP), an FDA-approved atypical antipsychotic, functions primarily as an
95 antagonist of dopamine receptors D2 and D3 (DRD2/DRD3) and is widely used in the
96 clinical management of schizophrenia and bipolar disorder. In our previous work, we
97 demonstrated the therapeutic potential of QTP in treating glioblastoma, one of the most
98 aggressive brain tumors, by targeting therapy-resistant cancer stem-like cells (21). Based

99 on these findings, we sought to investigate whether QTP could exert similar anti-tumor

100 effects when used in combination with radiotherapy or chemotherapeutic agents in TNBC.

Materials and Methods

TCGA data mining and analysis

Data from The Cancer Genome Atlas (TCGA) Invasive Breast Carcinoma cohort (assessed via cBioPortal on February 10, 2025) was used for this analysis. Expression data (RNA-Seq V2 RSEM Z scores) and overall survival data for DRD2 and DRD3 were retrieved. Only patients with available data for both gene expression and survival were included in the analysis (N=1980). Kaplan-Meier survival analysis was performed using a Z-score cut-off of 1.0, and the patients were stratified into subgroups based on expression levels: up-regulated, down-regulated, and unchanged. These stratified groups were then used to estimate overall survival differences.

Cell lines

The human SUM159-PT triple-negative breast cancer cell line was purchased from Asterand (Detroit, MI) and cultured in F12 Medium (Invitrogen, Carlsbad, CA) supplemented with 5 % fetal bovine serum (FBS), penicillin (100 units/ml), streptomycin (100 µg/ml), 5 µg/ml insulin (Eli Lilly, Indianapolis, IN), 0.1 % 1M HEPES buffer (Invitrogen) and 1 µg/ml hydrocortisone (Pfizer, New York, NY), under log-phase growth conditions. BT-549 and MDA-MB-231 breast cancer cell lines were obtained from Amrican Type Culture Collection (ATCC). MDA-MB-231 cells were cultured in Dulbecco's Modified Eagle Medium (DMEM; Thermo Fisher) with 10% FBS, and penicillin-streptomycin, while BT-549 cells were maintained in RPMI-1640 medium (Thermo Fisher) supplemented with 10% FBS, 1% penicillin-streptomycin, and insulin (0.023 IU/ml). All cell lines were grown

123 in a humidified incubator at 37 °C with 5 % CO2 and routinely tested for mycoplasma
124 infection (#G238, Applied biological Materials, Ferndale, WA). The unique identity of all
125 cell line was confirmed by DNA fingerprinting (Laragen, Culver City, CA).

126

127 *Drug treatment*

128 Quetiapine (#KS-1099, Key Organic) was dissolved at a stock concentration of 10 mM in
129 DMSO, and 1 μM, 2.5 μM, 5 μM, 10 μM, 20 μM were used. Paclitaxel (#S1150,
130 Selleckchem) was dissolved at a stock concentration of 5 mM in DMSO, and 1 nM, 5 nM,
131 10 nM were used. 5-fluorouracil (#S1209, Selleckchem) was dissolved at a stock
132 concentration of 10 mM in DMSO, and 0.5 μM, 1 μM, 5 μM were used. Doxorubicin
133 (#15007, Cayman Chemical) was dissolved at a stock concentration of 5 mM in DMSO,
134 and 5 nM, 10 nM, 20 nM were used.

135

136 *Quantitative Reverse Transcription-PCR*

137 Total RNA was isolated using TRIZOL Reagent (Invitrogen). cDNA synthesis was carried
138 out using the SuperScript Reverse Transcription IV (Invitrogen). Quantitative PCR was
139 performed in the QuantStudio™ 3 Real-Time PCR System (Applied Biosystems, Carlsbad,
140 CA, USA) using the PowerUp™ SYBRTM Green Master Mix (Applied Biosystems). C_t for
141 each gene was determined after normalization to GAPDH and $\Delta\Delta C_t$ was calculated
142 relative to the designated reference sample. Gene expression values were then set equal
143 to $2^{-\Delta\Delta Ct}$ as described by the manufacturer of the kit (Applied Biosystems). All PCR

144 primers were synthesized by Invitrogen with PPIA as the housekeeping gene (for primer
145 sequences see **Supplementary Table 1**).

146

147 *Clonogenic survival assay*

148 SUM159-PT, BT-549, and MDA-MB-231 cells were trypsinized and plated into 6-well
149 plates at a density of 100-200 cells per well. The following day, cells were treated with
150 either DMSO, QTP, chemotherapeutic drugs or QTP plus chemotherapeutic drugs at the
151 indicated concentrations. Culture media was refreshed every three days. After two weeks,
152 colonies were fixed and stained with 0.5% crystal violet. Colonies consisting of at least
153 50 cells were counted in each group and presented as percentage of colonies formed
154 relative to the number of cells initially plated.

155

156 *Mammosphere Formation Assay with Extreme Limiting Dilution Analysis (ELDA)*

157 SUM159-PT and BT-549 mammospheres were dissociated by TrypLE™ and plated into
158 96-well ultra-low attachment plates in mammosphere media (DMEM-F12, 10 ml/500 ml
159 B27 [Invitrogen], 5 μg/ml bovine insulin [Sigma], 4 μg/ml heparin [Sigma], 20 ng/ml basic
160 fibroblast growth factor [bFGF, Sigma], and 20 ng/ml epidermal growth factor [EGF,
161 Sigma]). For ELDA, cells were seeded at varying densities: 1 to 512 cells per well for 0
162 Gy conditions, 2 to 1024 cells per well for 4 Gy, and 4 to 2048 cells per well for 8 Gy. Cells
163 were treated with either QTP (10 μM) or DMSO solvent control one hour prior to receiving
164 a single dose of 0, 4, or 8 Gy radiation the next day. Growth factors (EGF and bFGF) were
165 replenished every 3 days. Mammospheres were cultured for 2-3 weeks, after which wells

166 containing spheres were counted. Results were expressed as the percentage of wells
167 with sphere formation relative to the initial number of cells plated.

168

169 *Irradiation*

170 Cells were irradiated at room temperature using an experimental X-ray irradiator (Gulmay
171 Medical Inc. Atlanta, GA) at a dose rate of 5.519 Gy/min. The X-ray beam was operated
172 at 300 kV and hardened using a 4 mm Be, a 3 mm Al, and a 1.5 mm Cu filter and calibrated
173 using NIST-traceable dosimetry. Corresponding controls were sham irradiated.

174

175 *Annexin V/PI Staining and Flow Cytometry*

176 SUM159-PT and BT-549 monolayer cells were plated onto 10-cm petri dishes and treated
177 with QTP (10 μM) one hour prior to receiving a single dose of 4 Gy irradiation the following
178 day. 72 hours post-irradiation, cells were harvested, washed twice with cold PBS, and
179 resuspended in 1X Annexin V binding buffer at a concentration of 1×10^6 cells/ml. For
180 each sample, 100 μl of cell suspension was incubated with 5 μl of FITC-conjugated
181 Annexin V and 5 μl of propidium iodide (PI, 50 μg/ml) for 15 minutes at room temperature
182 in the dark. Following incubation, 400 μl of binding buffer was added, and samples were
183 immediately analyzed using a BD LSR Fortessa flow cytometer (BD Bioscience, San Jose,
184 CA), acquiring a minimum of 50,000 events per sample. Data analysis were performed
185 using FlowJo v10 software. Cells positive for Annexin V and negative for PI were defined
186 as early apoptotic, double-positive cells as late apoptotic or necrotic, and double-negative
187 cells are viable cells.

188

189 *Cell Proliferation*

190 SUM159-PT and BT-549 monolayers were trypsinized and seeded at a density of 10,000
191 cells per 4-cm petri dish. The following day, cells were treated with either DMSO or QTP
192 (10 μM), with or without a single dose of 4 Gy radiation. Cell proliferation was assessed
193 by harvesting and counting cells on day 5, 10, 15, and 20 post-treatment.

194

195 *Migration/Invasion Assay*

196 Serum-starved SUM159-PT or BT-549 monolayers were trypsinized and plated onto
197 Transwell inserts (#08-771-12, Fisher Scientific) at a density of 1 x 10^5 cells per well. QTP
198 or solvent control (DMSO) was added to the medium in the bottom chamber containing
199 10% FBS. A negative control using 1% FBS medium was included to eliminate the FBS
200 gradient between the upper and lower chambers. After 16-24 hours of incubation, cells
201 were fixed with 10% formalin. Non-migrated cells on the upper side of the membrane
202 were gently removed with cotton swabs, while migrated cells on the lower side were
203 stained with 0.5% crystal violet. Images were captured using a digital microscope (BZ-
204 9000, Keyence, Itasca, IL) and quantified using Image J software.

205 For experiments involving irradiation, SUM159-PT or BT-549 monolayers were plated
206 onto 10-cm Petri dishes and treated with 10 μM QTP, with or without a single dose of 4
207 Gy irradiation. 48 hours post-irradiation, the cells were serum starved overnight. The
208 following day, cells were trypsinized and plated onto Transwell inserts at 1 x 10^5 cells per
209 well. The bottom chamber contained 10% FBS medium to create an FBS gradient that

210 promotes cell migration. After 16-24 hours, cells were fixed and stained with crystal violet
211 as described above.

212

213 γ-H2AX immunofluorescence staining

214 SUM159-PT monolayer cells were seeded onto the round glass coverslips at a density of
215 1 x 10^5 cells/well in the 6-well plate. The following day, cells were treated with DMSO or
216 QTP (10 μM), with or without a single dose of 4 Gy radiation. 6 hours and 24 hours post-
217 treatment, the coverslips were fixed, permeabilized, and blocked with 10% goat serum in
218 PBS for 1 hour at RT. The γ-H2AX primary antibody (Cell Signaling Technology, #9718s,
219 1:250) was then applied and incubated overnight at 4°C. The next day, the secondary
220 antibodies Alexa Fluor 594 Goat Anti-rabbit immunoglobulin G (IgG) (H/L) antibody
221 (1:1,000 (Invitrogen)) was applied for 60 min, with subsequent nuclear counterstaining
222 with Hoechst 33342 (Invitrogen, Cat# H3570, 1:5000). The sections were sealed with
223 VECTASHIELD® PLUS Antifade Mounting Medium (Vector Laboratories, Cat#H-1900)
224 and images were taken with a digital microscope (BZ-9000, Keyence, Itasca, IL).

225

226 *Statistics*

227 All data are represented as mean ± standard error mean of at least 3 biologically
228 independent experiments. A P value of < 0.05 in a 2-sided student t-test or ANOVA
229 indicated a statistically significant difference.

Results

Up-regulated DRD2 expression is associated with decreased overall survival in invasive breast cancer patients

To determine whether the expression levels of dopamine receptors DRD2 and DRD3 correlate with clinical outcomes in invasive breast cancer, we analyzed overall survival (OS) data from 1,980 invasive breast cancer patients within the TCGA Provisional dataset. Patients were stratified into three subgroups based on DRD2 and DRD3 expression levels (upregulated, downregulated, or unchanged), using a Z-score cutoff of ±1.0. Our analysis revealed that patients exhibiting upregulated DRD2 expression demonstrated significantly poorer median overall survival (111.10 months; p = 0.0245) compared to patients with unchanged DRD2 expression (157.83 months) **(Fig. 1a/b)**. In contrast, the median survival for patients with downregulated DRD2 expression (151.17 months) did not significantly differ from patients with normal expression (p = 0.801) **(Suppl. Fig. 1a/b)**. Furthermore, no significant difference in median survival was observed between patients with either upregulated or downregulated DRD3 expression and those with unchanged DRD3 expression levels **(Fig. 1c/d; Suppl. Fig. 1c/d)**.

Dopamine receptor expression in human triple-negative breast cancer cell lines under baseline and post-radiation conditions

We next examined the expression of dopamine receptors (DRD2 and DRD3) in established human TNBC cell lines. Cells were cultured both as monolayers and as mammospheres, the latter of which enriches for stem/progenitor cell populations.

252 Interestingly, expression levels of DRD2 and DRD3 were significantly elevated in
253 mammosphere cultures compared to their corresponding monolayer controls across all
254 three TNBC lines tested (SUM159-PT, BT-549, and MDA-MB-231) (**Fig. 2a**; black dashed
255 line indicates baseline). Given that radiation can alter the surface expression of certain
256 receptors, we also investigated DRD2 and DRD3 levels following exposure to single
257 doses of 0, 4, or 8 Gy radiation under both adherent and mammosphere conditions. At 24
258 hours post-irradiation, DRD2 and DRD3 expression showed slight increases. However,
259 these changes were not statistically significant **(Fig. 2b)**. Collectively, our results indicate
260 that dopamine receptors are enriched within TNBC stem/progenitor cell populations, and
261 their expression remains largely unaffected by sub-lethal radiation doses, suggesting
262 receptor stability in radioresistant cell populations.

263

264 *Quetiapine decreases clonogenicity and self-renewal in triple-negative breast cancer*

265 To evaluate the potential anti-tumor effects of QTP in TNBC, we first performed
266 clonogenic survival assays using all three TNBC lines (SUM159-PT, BT-549, and MDA-
267 MB-231). Treatment with QTP resulted in a significant, dose-dependent reduction in
268 colony formation capacity across all tested cell lines, and the effects seemed to reach a
269 plateau at approximately 10 μM concentration. These findings strongly suggest that QTP
270 has a robust inhibitory effect on the clonogenicity of tumor cells **(Fig. 2a-d)**. Next, we
271 examined whether QTP enhances cellular radiosensitivity by performing mammosphere-
272 forming assays with increasing doses of radiation (0, 2, 4, 6, and 8 Gy) using SUM159-
273 PT and BT-549 cells. Intriguingly, QTP treatment did not exhibit significant radiosensitizing
274 effects, as the surviving fraction of mammosphere remained largely unaffected by

275 combined radiation and QTP treatments compared to radiation alone **(Fig. 2e/f)**.
276 Microscopic examination of mammospheres revealed that QTP treatment resulted in
277 substantially fewer and smaller mammospheres compared to DMSO or radiation alone
278 groups **(Fig. 2g)**. Additionally, extreme limiting dilution analyses demonstrated that QTP
279 significantly reduced mammosphere-forming capacity and stem cell frequency, both in
280 sham-irradiated cells and in cells receiving single doses of 4 or 8 Gy radiation **(Fig. 2h-**
281 **k)**. Taken together, our results demonstrate that while QTP strongly suppresses
282 clonogenic growth and the self-renewal capacities of TNBC cells, it does not directly
283 increase tumor cell radiosensitivity.

284

285 *Quetiapine induces apoptosis and inhibits migratory capacity in TNBC cells*

286 To elucidate the cellular mechanisms underlying the anti-tumor effects of QTP in TNBC
287 cells, we cultured SUM159-PT and BT-549 cells in monolayers and treated them with 10
288 μM QTP, either alone or in combination with a single dose of 4 Gy radiation. Cell viability
289 and proliferation were monitored at a regular interval (every 5 days) over a 20-day period.
290 Notably, QTP treatment resulted in a significant reduction in cell proliferation at day 10
291 post-treatment in SUM159-PT cells **(Fig. 4a)**, while in BT-549 cells, the inhibitory effects
292 were pronounced as early as day 5 **(Fig. 4b)**. Furthermore, combined treatment with QTP
293 and radiation markedly reduced cell viability compared to radiation alone in both lines
294 **(Fig. 4c/d)**.

295

296 To determine whether the observed inhibition of cell proliferation resulted from induction
297 of cell apoptosis, we conducted Annexin V/PI staining followed by flow cytometry analysis.
298 Our results revealed that QTP treatment significantly reduced the percentage of viable
299 cells and markedly increased the proportion of early apoptotic cells (defined as the
300 Annexin V-positive/PI-negative). Additionally, there was a substantial increase in late
301 apoptotic or necrotic populations (Annexin V-positive/PI-positive) **(Fig. 4e-g)**.

302

303 TNBC is known for its aggressive behavior, often spreading more rapidly and frequently
304 than other breast cancer subtypes, which leads to a high risk of early metastasis. To
305 investigate whether QTP impacts the migratory/invasive properties of TNBC cells, we
306 performed transwell migration assay using two experimental approaches **(Fig. 4h)**. In the
307 first setup, QTP was added to the lower chamber to assess its effect as a chemoattractant
308 inhibitor. Here, we demonstrated that QTP significantly reduced the migratory capacity of
309 both SUM159-PT and BT-549 cells, as evidenced by a decreased number of cells
310 penetrating through the transwell membrane **(Fig. 4i-k)**. In the second approach, cells
311 were pre-treated with QTP alone or in combination with a single dose of 4 Gy radiation,
312 prior to seeding. The pre-treated cells displayed markedly impaired migration capacity
313 compared to untreated and radiation-only controls **(Fig. 4l-n)**. These findings suggest that
314 QTP effectively inhibits TNBC cell motility independently and in combination with radiation,
315 highlighting its potential to suppress metastatic progression.

316

317 *Quetiapine induces DNA double-strand breaks and impairs DNA repair in TNBC cells*

318 Based on our observations that QTP reduces cell viability, impairs self-renewal, and
319 suppresses migratory potential in TNBC cells, we next sought to explore whether its anti-
320 tumor effects are associated with the induction of genomic instability and disruption of
321 DNA repair mechanisms. Given that radiation therapy primarily exerts its cytotoxic effects
322 through the induction of DNA double-strand breaks (DSBs), and the ability to repair such
323 damage is essential for tumor cell survival and therapy resistance. In order to examine
324 whether QTP contributes to DNA damage or interferes with the repair process, we
325 evaluated the formation and resolution of γ-H2AX foci, a widely accepted marker of DSBs,
326 at 6 hours and 24 hours following exposure to a single dose of 4 Gy radiation, in the
327 presence or absence of QTP using SUM159-PT cells. At 6 hours post-radiation, QTP-
328 treated cells exhibited a marked increase in γ-H2AX positive cells compared to both
329 DMSO control and cells treated with radiation alone, suggesting that QTP enhances the
330 induction of DNA damage in TNBC cells **(Fig. 5a/b)**. Notably, while radiation-induced γ-
331 H2AX foci typically resolve by 24 hours post-radiation as a result of efficient DNA repair,
332 QTP-treated cells displayed a persistent γ-H2AX signal at this later time point **(Fig. 5c/d)**.
333 This indicates a significant delay in DNA repair and suggests that QTP may impair the
334 resolution of DSBs.

335

336 *Anti-tumor effects of QTP and chemotherapeutic agents in TNBC cells*

337 To evaluate the potential of QTP as a combination therapy in TNBC, we investigated
338 whether it could enhance the efficacy of standard chemotherapeutic agents commonly
339 used in clinical settings. Specifically, we tested QTP in combination with doxorubicin
340 (DOX), paclitaxel (TAXOL), and 5-fluorouracil (5-FU) in SUM159-PT cells. Given the high

341 potency of QTP at 10 μM, we reduced its concentration to 5 μM to better assess
342 synergistic interactions. Clonogenic survival assays revealed a substantial reduction in
343 colony-forming ability when QTP was combined with low doses of 5-FU (0.5 μM) **(Fig. 6a)**
344 or TAXOL (0.5 μM) **(Fig. 6b)**, indicating enhanced cytotoxicity beyond single-agent
345 treatments. Notably, the combination of QTP and DOX demonstrated a clear dose-
346 dependent suppression of clonogenicity **(Fig. 6c)**.

347

348 To confirm the broader applicability of this synergy, we extended the analysis to two
349 additional TNBC cell lines, BT-549 and MDA-MB-231. In BT-549 cells, the combined
350 treatment of 5 μM QTP with 20 nM DOX eliminated colony formation **(Fig. 6d)**. Similarly,
351 MDA-MB-231 cells showed a near-complete loss of clonogenic potential when treated
352 with 5 μM QTP in combination with either 10 nM or 20 nM DOX **(Fig. 6e)**. These consistent
353 findings across multiple TNBC lines support the conclusion that QTP significantly
354 sensitizes TNBC cells to doxorubicin and other chemotherapeutic agents.

355

356 Furthermore, we examined whether this synergistic interaction extended to the self-
357 renewal capacity of TNBC cells using the mammosphere-forming assay. The combination
358 of QTP and DOX completely abolished sphere formation in BT-549 cells **(Fig. 6f)**, and
359 similar effects were observed in SUM159-PT cells treated with 10 μM QTP plus DOX **(Fig.**
360 **6g)**. These results indicate that QTP not only enhances the cytotoxic effects of
361 chemotherapy on bulk tumor cells but also effectively targets cancer stem-like cells,

362 supporting its potential as a valuable adjuvant to conventional chemotherapy in the
363 treatment of TNBC.
364

365 **Discussion**

366 The psychiatric drug quetiapine, a second-generation atypical antipsychotic commonly
367 used for the treatment of schizophrenia and bipolar disorder, has recently demonstrated
368 promising anti-tumor effects in several preclinical cancer models (21, 23). Despite these
369 encouraging results, its therapeutic efficacy has not yet been evaluated in triple-negative
370 breast cancer, a highly aggressive subtype characterized by limited treatment options and
371 poor patient prognosis. In this study, we report, for the first time, that QTP not only inhibits
372 tumor clonogenicity and self-renewal but also enhances the efficacy of both radiation and
373 chemotherapeutic agents in multiple TNBC cell models.

374

375 More importantly, these effects are observed when QTP is used alone and are further
376 amplified in combination with clinically relevant treatments, such as ionizing radiation,
377 doxorubicin, paclitaxel, and 5-fluorouracil. This suggests a synergistic or additive
378 interaction between QTP and standard-of-care therapies, potentially offering a new
379 combination strategy for this highly aggressive subtype. Mechanistically, we show that
380 QTP induces apoptosis and promotes the accumulation of DNA double-strand breaks.
381 Notably, QTP also delays the resolution of γ-H2AX foci over time, suggesting that it
382 disrupts the DNA damage response and impairs DNA repair process. This is particularly
383 significant in the context of radiotherapy or genotoxic chemotherapy, where DNA repair
384 pathways are critical for tumor cell survival (24, 25). Additionally, QTP suppresses the
385 bulk tumor cell migration, as well as the cells that survive sublethal radiation, indicating
386 its potential to prevent metastatic progression and recurrence.

These observations are in line with previous reports on the anti-tumor activity of dopamine receptor antagonists (15, 26, 27). Prior studies have demonstrated that other antipsychotic agents such as thioridazine and domperidone could target cancer stem-like cells and reduce self-renewal in TNBC via DRD2 inhibition and subsequent suppression of downstream pathways such as STAT3 and JAK/STAT signaling (26, 27). Our findings extend these insights by identifying QTP, a DRD2/DRD3 antagonist with a well-established clinical safety profile, as a novel agent capable of replicating these effects while offering additional therapeutic advantages. Unlike previous studies that focused solely on monotherapy, our work highlights the potential of QTP as a promising adjuvant therapeutic agent when combined with radiation and chemotherapy.

TNBC patients have a higher likelihood of developing brain metastases compared to those with hormone receptor-positive subtypes. These metastases not only occur more frequently but also tend to develop earlier in the course of the disease (28). Once brain involvement is detected, the prognosis is generally poor, with median overall survival typically ranging from 4 to 9 months, making it a major driver of morbidity and mortality in patients with metastatic TNBC (29-31). Beyond the physical challenges posed by metastasis, many TNBC patients also suffer from the neurological and psychological side effects of systemic chemotherapy, including cognitive dysfunction (“chemo brain”), anxiety, depression, and sleep disturbances. These symptoms can severely compromise quality of life and hinder adherence to treatment regimens (32-34). Here QTP presents as a compelling candidate for repurposing in oncology due to several favorable

410 pharmacological properties. It readily crosses the blood-brain barrier, has a well-
411 documented safety profile with a low incidence of severe side effects, and is widely used
412 in clinical practice for managing psychiatric conditions. In previous studies, QTP has been
413 shown to effectively eliminate glioma-initiating cells, highlighting its capacity to act against
414 therapy-resistant cancer stem-like cells within the brain (21). These findings raise the
415 possibility that QTP may also exhibit therapeutic efficacy against TNBC brain metastases.
416 This multifunctional profile could be advantageous in managing the complex needs of
417 TNBC patients with central nervous system (CNS) involvement, and it warrants further
418 investigation in preclinical and clinical settings.

419

420 Despite these promising findings, our study has several limitations. Most notably, all
421 experiments were conducted *in vitro*, and the complexities of the tumor microenvironment,
422 drug metabolism, and immune interactions could potentially influence its therapeutic
423 efficacy *in vivo*. Future studies are needed to evaluate its efficacy in TNBC xenograft or
424 patient-derived orthotopic mouse models to confirm its anti-tumor and anti-metastatic
425 potential in a physiologically relevant context. Furthermore, although QTP is considered
426 to act as a DRD2/DRD3 antagonist, it interacts with several other receptors (e.g.,
427 serotonin and adrenergic receptors), and their contributions to the observed phenotypes
428 remain to be explored. Lastly, the molecular pathways downstream of DRD2/DRD3 that
429 mediate QTP's effects in TNBC warrant further mechanistic study.

430

431 **Conclusions**

432 In conclusion, our study provides new insight into the anti-tumor properties of QTP in
433 TNBC and identifies it as a promising candidate for combination therapies. By impairing
434 DNA repair, inducing apoptosis, and suppressing migratory and stem-like features of
435 TNBC cells, QTP has the great potential to overcome some of the major therapeutic
436 challenges in this aggressive breast cancer subtype. These findings lay the groundwork
437 for future preclinical and clinal studies aimed at repurposing QTP as an adjuvant
438 treatment strategy for TNBC, potentially improving patient outcomes through a more cost-
439 effective, well-tolerated therapeutic approach.

440

441 **List of Abbreviations**

442 TNBC: triple-negative breast cancer; QTP: quetiapine; ER: estrogen receptor; PR:
443 progesterone receptor; HER2: human epidermal growth factor receptor 2; DRD2:
444 dopamine receptors D2; DRD3: dopamine receptors D3; DRD4: dopamine receptors D4;
445 PI: propidium iodide; TAXOL: paclitaxel; DOX: doxorubicin; 5-FU: 5-fluorouracil; DSBs:
446 DNA double-strand breaks; CNS: central nervous system.

447

448 **ORCHID information:** Ling He: 0000-0002-8692-7530; Frank Pajonk: 0000-0003-4067-
449 9751.

450

451 **Author contributions:** FP and LH conceived and designed the experiments. LH and PJ
452 performed most of the experiments, AK, AI, and MS helped with some experiments. LH
453 drafted the original manuscript, FP edited and revised the draft. All authors read and
454 approved the final manuscript.

455

456 **Funding**

457 This work was supported by UCLA JCCC postdoctoral fellowship to LH. FP was supported
458 by grants from the *National Cancer Institute* (R01CA260886, R01CA281682).

459

460 **Availability of data and materials**

All data relevant to the study are included in the article or uploaded as supplementary information.

Consent for publication

The content of this paper has not been submitted to any other scientific publications. All the authors have declared that no financial conflict of interest exists. All authors have approved the submission of this work for publication in Breast Cancer Research.

Competing interests

The authors declare no competing interests.

472 **Figure Legends**

473 **Figure 1. Evaluation of overall survival based on DRD2 and DRD3 signatures in**
474 **invasive breast cancer patients.**

475 **(a)** Kaplan-Meier analysis of overall survival (OS) in invasive breast cancer patients
476 stratified by DRD2 mRNA expression levels. The red line represents patients with
477 upregulated DRD2 expression, while the blue line indicates those with unchanged
478 expression. Patients in the DRD2 upregulated group exhibited significantly worse OS
479 compared to the unchanged group (log-rank test, p=0.0245). The number of patients at
480 risk is displayed below the Kaplan-Meier curve. **(b)** Summary table showing the total
481 number of cases, deceased cases, and median survival of patients with either
482 upregulated or unchanged DRD2 expression. **(c)** Kaplan-Meier analysis of OS in invasive
483 breast cancer patients based on DRD3 mRNA expression levels. The red line denotes
484 patients with upregulated DRD3 expression, while the blue line represents those with
485 unchanged expression. OS in the DRD3 upregulated subgroup was not significantly
486 different from the unchanged group (log-rank test, p=0.0694). The number of patients at
487 risk is displayed below the Kaplan-Meier curve. **(d)** Summary table presenting the total
488 number of cases, deceased cases, and median survival of patients with upregulated or
489 unchanged DRD3 expression.

490

491 **Figure 2. Dopamine receptor expression in human triple-negative breast cancer cell**
492 **lines under baseline and post-radiation conditions.**

493 **(a)** Relative expression levels of DRD2 and DRD3 in mammospheres compared to their
494 corresponding monolayers in SUM159-PT, BT-549, and MDA-MB-231 triple-negative
495 breast cancer cell lines, as assessed by qRT-PCR. **(b/c)** DRD2 and DRD3 expression
496 levels in mammospheres and monolayers of SUM159-PT, BT-549, and MDA-MB-231
497 following exposure to a single dose of 4 Gy or 8 Gy radiation, measured at 24 hours post-
498 treatment. All experiments have been performed with at least 3 biological independent
499 repeats. *P*-values were calculated using one-way ANOVA.

500

501 **Figure 3. Quetiapine decreases clonogenicity and self-renewal in triple-negative**
502 **breast cancer.**

503 **(a-c)** Clonogenic assays performed on patient-derived triple-negative breast cancer cells
504 (SUM159-PT, BT-549, and MDA-MB231) treated with quetiapine at 1, 2.5, 5, 10, or 20
505 μM, or with DMSO (solvent control). **(d)** The colony number was counted and presented
506 as the percentage relative to the initial number of cells plated. **(e/f)** Surviving fraction of
507 SUM159-PT and BT-549 mammospheres treated with quetiapine at 1, 5, or 10 μM. **(g)**
508 Representative images of SUM159-PT and BT-549 mammospheres treated with
509 quetiapine (10 μM), with or without a single 4 Gy or 8 Gy radiation dose. **(h)**
510 Mammosphere forming capacity of SUM159-PT and BT-549 spheres treated with
511 quetiapine (10 μM), with or without a single 4 Gy or 8 Gy radiation dose. **(i/j)** Extreme
512 Limiting Dilution Analysis (ELDA) plots showing the relationship between the number of
513 cells plated per well and the fraction of negative wells (no colonies) in SUM159-PT and
514 BT-549 mammospheres following the combination of radiation and quetiapine. **(k)**
515 Estimated stem cell frequencies and 95% confidence intervals in each treatment group.

516 All experiments have been performed with at least 3 biological independent repeats. *P*-
517 values were calculated using one-way ANOVA.

518

519 **Figure 4. Quetiapine promotes apoptosis and reduces the migratory capacity of**
520 **TNBC cells.**

521 **(a-d)** Quantification of cell number and viability in SUM159-PT and BT-549 cells treated
522 with 10 μM QTP, with or without a single dose of 4 Gy radiation, assessed on days 5, 10,
523 15, and 20 post-treatment. **(e)** Representative Annexin V/PI dot plots of SUM159-PT and
524 BT-549 cells treated with QTP (10 μM), with or without a single 4 Gy dose of radiation,
525 analyzed 72 hours post-treatment. **(f/g)** Quantification of viable, early apoptotic, and late
526 apoptotic/necrotic cell populations. **(h)** Schematic illustration of two transwell migration
527 assay setups. **(i-k)** Transwell invasion assay of SUM159-PT and BT-549 cells with QTP
528 (10 μM) added to the lower chamber of an 8-μm pore insert. Media containing 1% FBS
529 and 10% FBS served as negative and positive control, respectively. Migrated cells were
530 quantified per high-power field using Image J. **(l-n)** Invasion assay of SUM159-PT and
531 BT-549 cells pretreated with QTP (10 μM) for 48 hours, with or without a single dose of 4
532 Gy radiation, followed by migration analysis. All experiments have been performed with
533 at least 3 biological independent repeats. *P*-values were calculated using one-way
534 ANOVA. * *p*-value < 0.05, ** *p*-value < 0.01, *** *p*-value < 0.001, **** *p*-value < 0.0001.

535

536 **Figure 5. Quetiapine induces DNA double-strand breaks and delays DNA repair in**
537 **TNBC cells.**

538 **(a)** Representative immunofluorescence images of γ-H2AX staining in SUM159-PT cells
539 treated with 10 μM QTP, with or without a single dose of 4 Gy radiation, analyzed 6 hours
540 post-radiation. **(b)** Quantification of γ-H2AX-positive cells per high-power field using
541 Image J. **(c/d)** Representative γ-H2AX immunofluorescence images and corresponding
542 quantification at 24 hours post-radiation under the same treatment conditions. All
543 experiments have been performed with at least 3 biological independent repeats. *P*-
544 values were calculated using one-way ANOVA. * *p*-value < 0.05, ** *p*-value < 0.01, *** *p*-
545 value < 0.001, **** *p*-value < 0.0001.

546

547 **Figure 6. Anti-tumor effects of quetiapine and chemotherapeutic agents in TNBC**
548 **cells.**

549 **(a-c)** Quantification of plating efficiency in SUM159-PT cells treated with 5 μM QTP in
550 combination with increasing concentrations of 5-fluorouracil (5-FU), paclitaxel (TAXOL),
551 or doxorubicin (DOX), assessed via clonogenic survival assays. **(d/e)** Clonogenic survival
552 of BT-549 and MDA-MB-231 cells treated with 5 μM QTP in combination with 5 nM, 10
553 nM, or 20 nM DOX. **(f/g)** Mammosphere-forming assays of BT-549 and SUM159-PT cells
554 treated with varying doses of QTP in combination with DOX to evaluate effects on self-
555 renewal. All experiments have been performed with at least 3 biological independent
556 repeats. *P*-values were calculated using two-way ANOVA. * *p*-value < 0.05, ** *p*-value <
557 0.01, *** *p*-value < 0.001, **** *p*-value < 0.0001.

558

559

Reference:

1. Siegel RL, Kratzer TB, Giaquinto AN, Sung H, Jemal A. Cancer statistics, 2025. CA Cancer J Clin. 2025;75(1):10-45.
2. Almansour NM. Triple-Negative Breast Cancer: A Brief Review About Epidemiology, Risk Factors, Signaling Pathways, Treatment and Role of Artificial Intelligence. Front Mol Biosci. 2022;9:836417.
3. Cleator S, Heller W, Coombes RC. Triple-negative breast cancer: therapeutic options. Lancet Oncol. 2007;8(3):235-44.
4. Zagami P, Carey LA. Triple negative breast cancer: Pitfalls and progress. NPJ Breast Cancer. 2022;8(1):95.
5. Yin L, Duan JJ, Bian XW, Yu SC. Triple-negative breast cancer molecular subtyping and treatment progress. Breast Cancer Res. 2020;22(1):61.
6. Dent R, Trudeau M, Pritchard KI, Hanna WM, Kahn HK, Sawka CA, et al. Triple-negative breast cancer: clinical features and patterns of recurrence. Clin Cancer Res. 2007;13(15 Pt 1):4429-34.
7. Dent R, Hanna WM, Trudeau M, Rawlinson E, Sun P, Narod SA. Pattern of metastatic spread in triple-negative breast cancer. Breast Cancer Res Treat. 2009;115(2):423-8.
8. Won KA, Spruck C. Triple-negative breast cancer therapy: Current and future perspectives (Review). Int J Oncol. 2020;57(6):1245-61.
9. Lee J. Current Treatment Landscape for Early Triple-Negative Breast Cancer (TNBC). J Clin Med. 2023;12(4).

582 10. Luond F, Tiede S, Christofori G. Breast cancer as an example of tumour
583 heterogeneity and tumour cell plasticity during malignant progression. Br J Cancer.
584 2021;125(2):164-75.
585 11. Fultang N, Chakraborty M, Peethambaran B. Regulation of cancer stem cells in
586 triple negative breast cancer. Cancer Drug Resist. 2021;4(2):321-42.
587 12. Bromberg-Martin ES, Matsumoto M, Hikosaka O. Dopamine in motivational control:
588 rewarding, aversive, and alerting. Neuron. 2010;68(5):815-34.
589 13. Speranza L, di Porzio U, Viggiano D, de Donato A, Volpicelli F. Dopamine: The
590 Neuromodulator of Long-Term Synaptic Plasticity, Reward and Movement Control. Cells.
591 2021;10(4).
592 14. Ahangari G, Norioun H. The dual role of dopamine and serotonin in cancer
593 progression and inflammation: Mechanisms and therapeutic potential. Neuroscience.
594 2025;569:184-94.
595 15. Moura C, Vale N. The Role of Dopamine in Repurposing Drugs for Oncology.
596 Biomedicines. 2023;11(7).
597 16. Jayachandran P, Battaglin F, Strelez C, Lenz A, Algaze S, Soni S, et al. Breast
598 cancer and neurotransmitters: emerging insights on mechanisms and therapeutic
599 directions. Oncogene. 2023;42(9):627-37.
600 17. Rosas-Cruz A, Salinas-Jazmin N, Velazquez MAV. Dopamine Receptors in Cancer:
601 Are They Valid Therapeutic Targets? Technol Cancer Res Treat.
602 2021;20:15330338211027913.
603 18. Wang X, Wang ZB, Luo C, Mao XY, Li X, Yin JY, et al. The Prospective Value of
604 Dopamine Receptors on Bio-Behavior of Tumor. J Cancer. 2019;10(7):1622-32.

605 19. Weissenrieder JS, Neighbors JD, Mailman RB, Hohl RJ. Cancer and the
606 Dopamine D(2) Receptor: A Pharmacological Perspective. J Pharmacol Exp Ther.
607 2019;370(1):111-26.
608 20. Bhat K, Saki M, Vlashi E, Cheng F, Duhachek-Muggy S, Alli C, et al. The dopamine
609 receptor antagonist trifluoperazine prevents phenotype conversion and improves survival
610 in mouse models of glioblastoma. Proc Natl Acad Sci U S A. 2020;117(20):11085-96.
611 21. Bhat K, Saki M, Cheng F, He L, Zhang L, Ioannidis A, et al. Dopamine Receptor
612 Antagonists, Radiation, and Cholesterol Biosynthesis in Mouse Models of Glioblastoma.
613 J Natl Cancer Inst. 2021;113(8):1094-104.
614 22. Li H, Li J, Yu X, Zheng H, Sun X, Lu Y, et al. The incidence rate of cancer in patients
615 with schizophrenia: A meta-analysis of cohort studies. Schizophr Res. 2018;195:519-28.
616 23. Su CM, Lin SS, Wang HC, Hsu FT, Chung JG, Hsu LC. The inhibitory effect and
617 mechanism of quetiapine on tumor progression in hepatocellular carcinoma in vivo.
618 Environ Toxicol. 2022;37(1):92-100.
619 24. Huang R, Zhou PK. DNA damage repair: historical perspectives, mechanistic
620 pathways and clinical translation for targeted cancer therapy. Signal Transduct Target
621 Ther. 2021;6(1):254.
622 25. Huang RX, Zhou PK. DNA damage response signaling pathways and targets for
623 radiotherapy sensitization in cancer. Signal Transduct Target Ther. 2020;5(1):60.
624 26. Tegowski M, Fan C, Baldwin AS. Thioridazine inhibits self-renewal in breast cancer
625 cells via DRD2-dependent STAT3 inhibition, but induces a G(1) arrest independent of
626 DRD2. J Biol Chem. 2018;293(41):15977-90.

627 27. Shakya R, Byun MR, Joo SH, Chun KS, Choi JS. Domperidone Exerts Antitumor
628 Activity in Triple-Negative Breast Cancer Cells by Modulating Reactive Oxygen Species
629 and JAK/STAT3 Signaling. Biomol Ther (Seoul). 2023;31(6):692-9.
630 28. Saraf A, Grubb CS, Hwang ME, Tai CH, Wu CC, Jani A, et al. Breast cancer
631 subtype and stage are prognostic of time from breast cancer diagnosis to brain metastasis
632 development. J Neurooncol. 2017;134(2):453-63.
633 29. Lin NU, Claus E, Sohl J, Razzak AR, Arnaout A, Winer EP. Sites of distant
634 recurrence and clinical outcomes in patients with metastatic triple-negative breast cancer:
635 high incidence of central nervous system metastases. Cancer. 2008;113(10):2638-45.
636 30. Kaplan MA, Isikdogan A, Koca D, Kucukoner M, Gumusay O, Yildiz R, et al.
637 Biological subtypes and survival outcomes in breast cancer patients with brain
638 metastases (study of the Anatolian Society of Medical Oncology). Oncology.
639 2012;83(3):141-50.
640 31. Gao C, Wang F, Suki D, Strom E, Li J, Sawaya R, et al. Effects of systemic therapy
641 and local therapy on outcomes of 873 breast cancer patients with metastatic breast
642 cancer to brain: MD Anderson Cancer Center experience. Int J Cancer. 2021;148(4):961-
643 70.
644 32. Anand U, Dey A, Chandel AKS, Sanyal R, Mishra A, Pandey DK, et al. Cancer
645 chemotherapy and beyond: Current status, drug candidates, associated risks and
646 progress in targeted therapeutics. Genes Dis. 2023;10(4):1367-401.
647 33. Dubey A, Agrawal S, Agrawal V, Dubey T, Jaiswal A. Breast Cancer and the Brain:
648 A Comprehensive Review of Neurological Complications. Cureus. 2023;15(11):e48941.

649 34. Cerulla N, Arcusa A, Navarro JB, de la Osa N, Garolera M, Enero C, et al. Cognitive
650 impairment following chemotherapy for breast cancer: The impact of practice effect on
651 results. J Clin Exp Neuropsychol. 2019;41(3):290-9.

652

Figure 1.

a

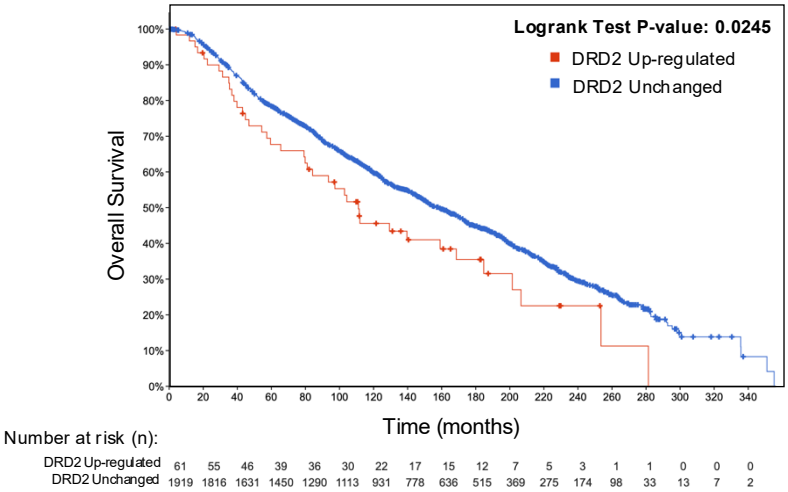

b

	Number of cases, Total	Number of cases, Deceased	Median months survival (95% CI)
Cases with high-expression in **DRD2** gene	61	40	111.10
Cases without alteration in **DRD2** gene	1919	1103	157.83

c

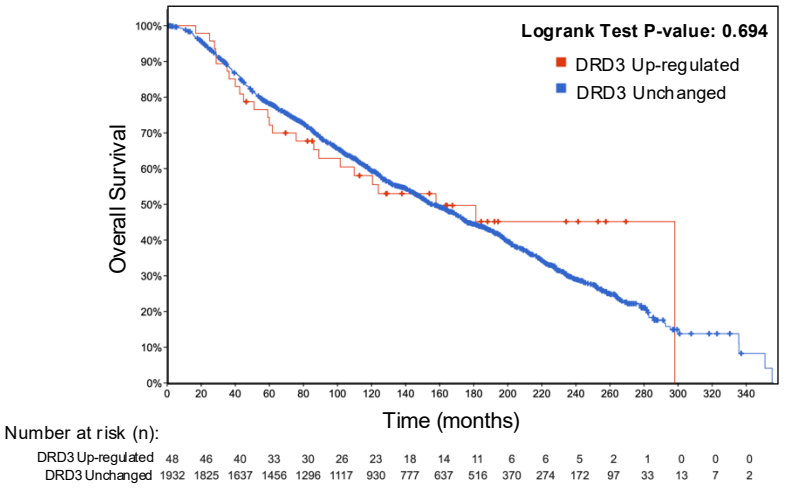

d

	Number of cases, Total	Number of cases, Deceased	Median months survival (95% CI)
Cases with high-expression in **DRD3** gene	48	24	157.83
Cases without alteration in **DRD3** gene	1932	1119	155.73

Figure 2.

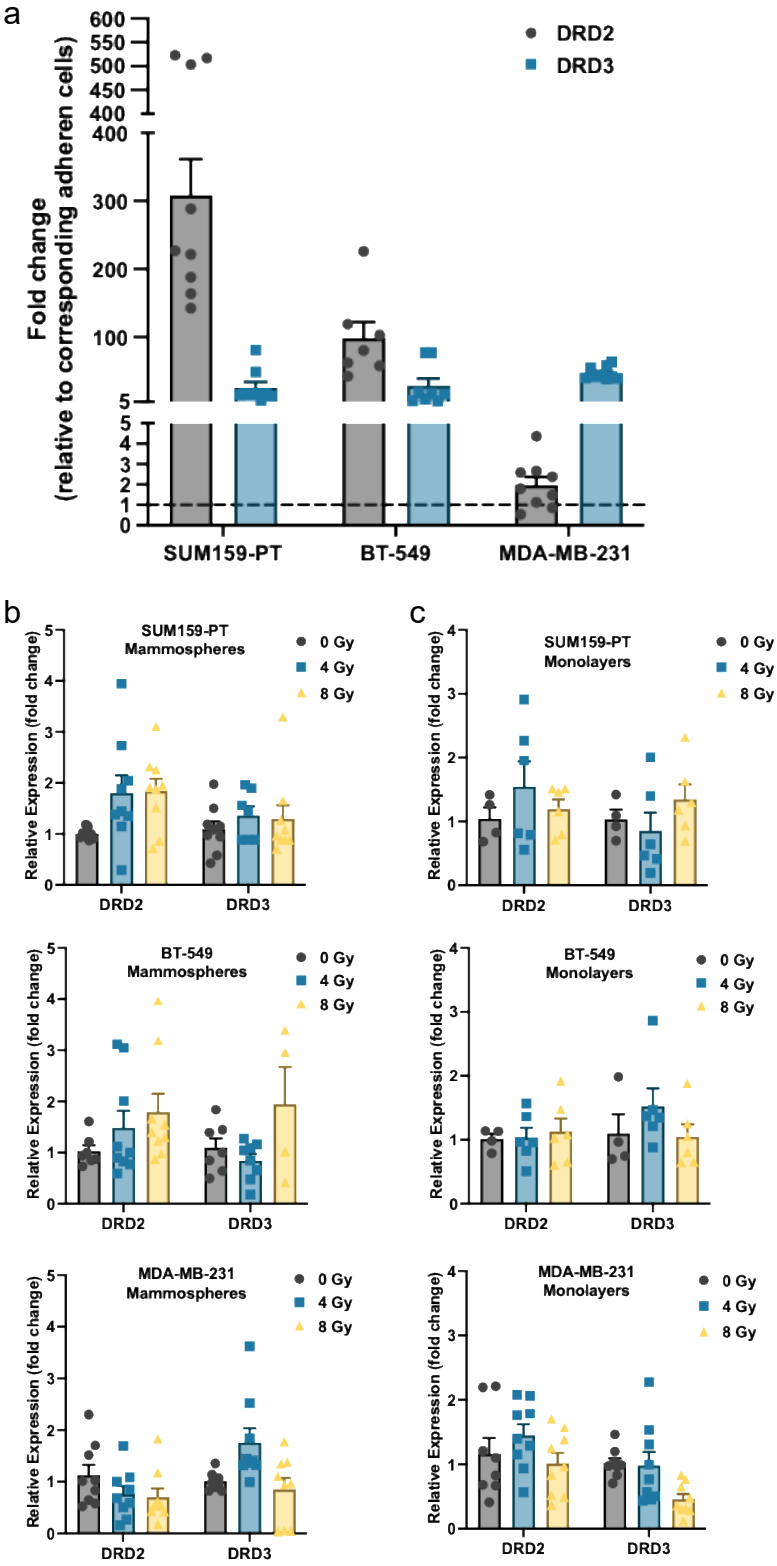
a
Fold change
(relative to corresponding adheren cells)
DRD2
DRD3
SUM159-PT
BT-549
MDA-MB-231
b
SUM159-PT
Mammospheres
BT-549
Mammospheres
MDA-MB-231
Mammospheres
c
SUM159-PT
Monolayers
BT-549
Monolayers
MDA-MB-231
Monolayers
0 Gy
4 Gy
8 Gy
Relative Expression (fold change)
DRD2
DRD3

Figure 3.

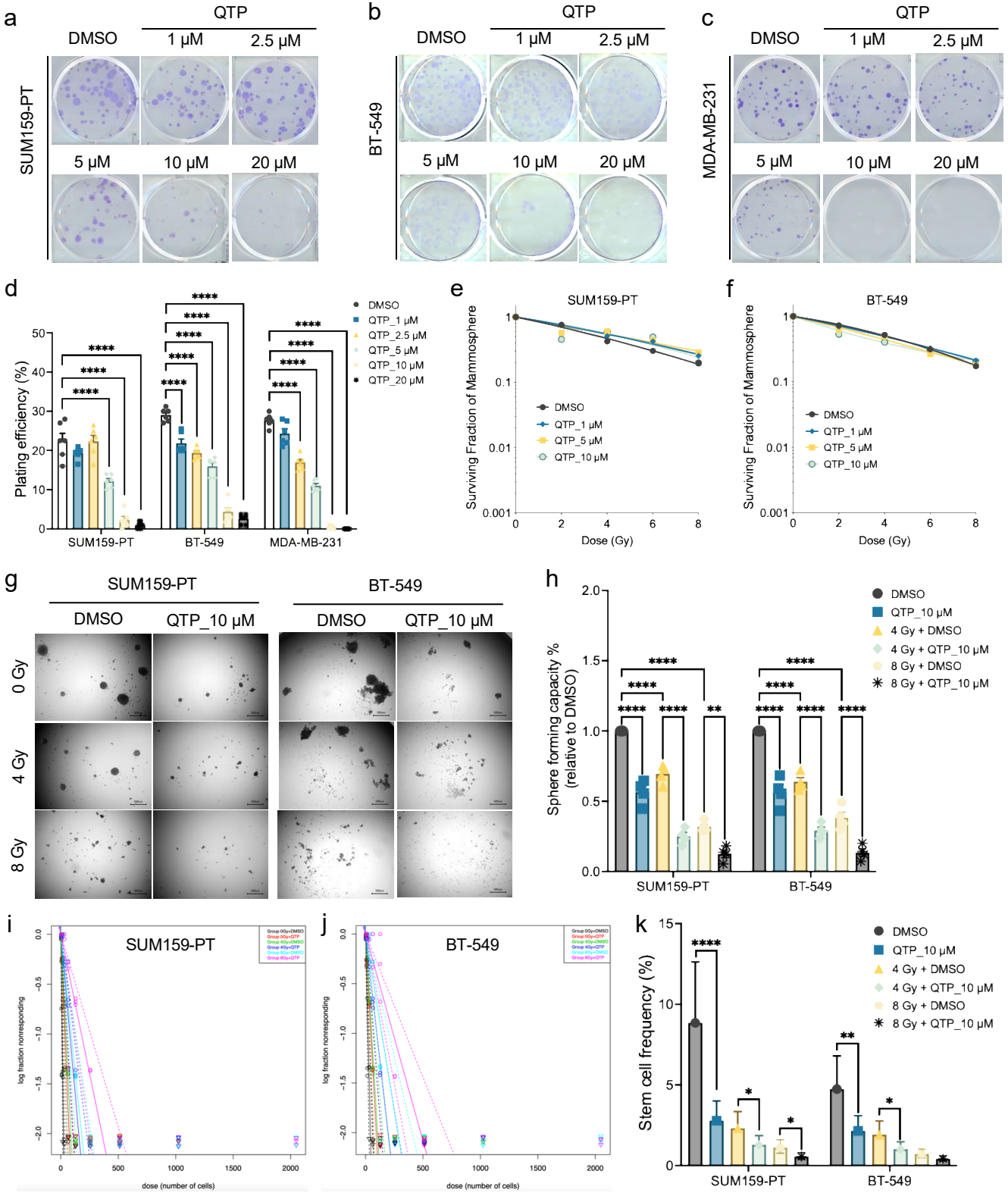
a
QTP
DMSO
1 μM
2.5 μM
SUM159-PT
5 μM
10 μM
20 μM
b
BT-549
c
MDA-MB-231
d
Plating efficiency (%)
DMSO
QTP_1 μM
QTP_2.5 μM
QTP_5 μM
QTP_10 μM
QTP_20 μM
SUM159-PT
BT-549
MDA-MB-231
e
Surviving Fraction of Mammosphere
Dose (Gy)
f
g
0 Gy
4 Gy
8 Gy
h
Sphere forming capacity % (relative to DMSO)
4 Gy + DMSO
4 Gy + QTP_10 μM
8 Gy + DMSO
8 Gy + QTP_10 μM
i
j
log fraction nonresponding
dose (number of cells)
k
Stem cell frequency (%)

Figure 4.

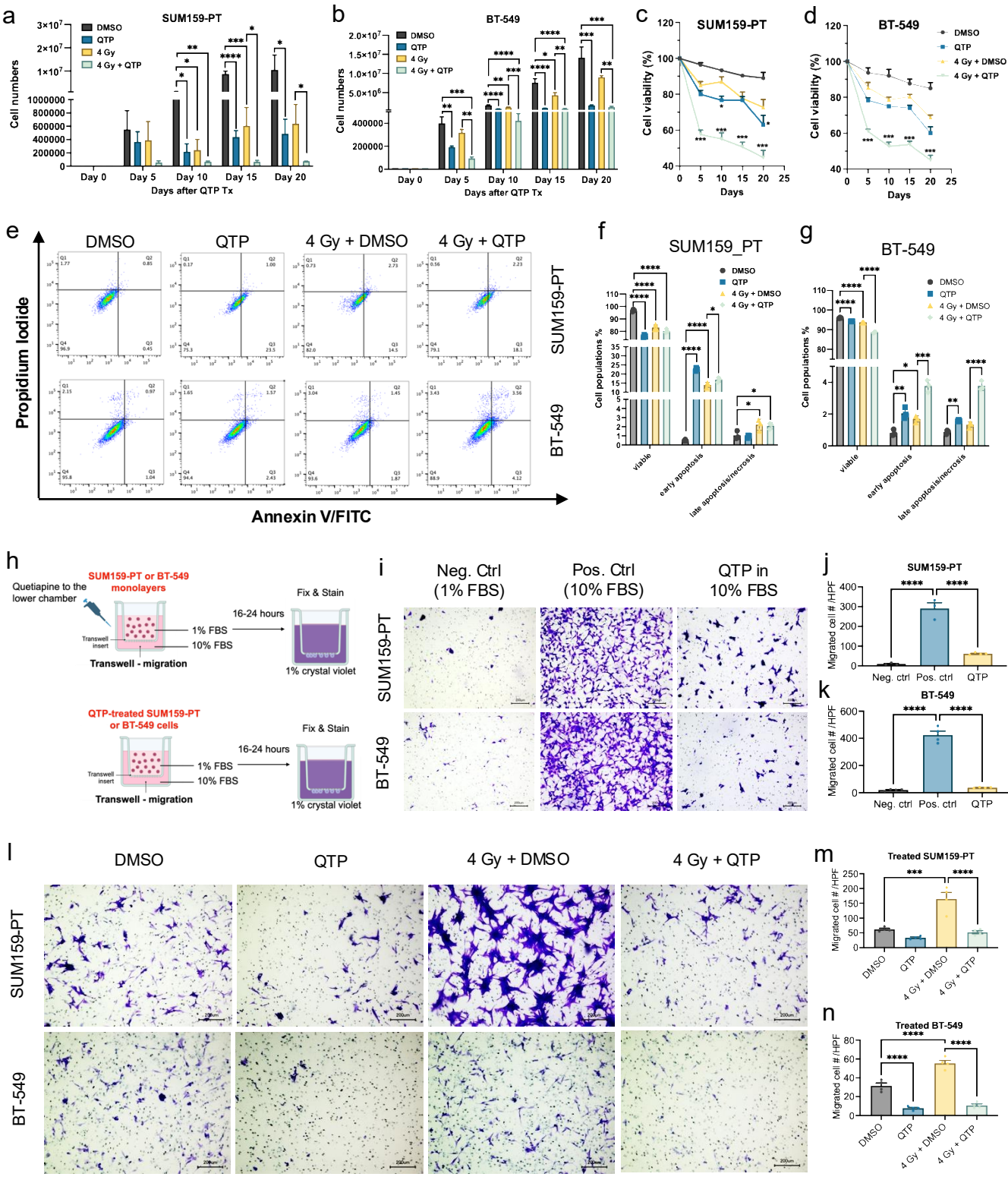
a
SUM159-PT
DMSO
QTP
4 Gy
4 Gy + QTP
Cell numbers
Days after QTP Tx
Day 0
Day 5
Day 10
Day 15
Day 20
b
BT-549
c
SUM159-PT
Cell viability (%)
Days
d
BT-549
e
DMSO
QTP
4 Gy + DMSO
4 Gy + QTP
Propidium Iodide
Annexin V/FITC
SUM159-PT
BT-549
f
SUM159_PT
Cell populations %
viable
early apoptosis
late apoptosis/necrosis
g
BT-549
h
SUM159-PT or BT-549 monolayers
Quetiapine to the lower chamber
Transwell insert
Transwell - migration
1% FBS
10% FBS
16-24 hours
Fix & Stain
1% crystal violet
QTP-treated SUM159-PT or BT-549 cells
i
Neg. Ctrl (1% FBS)
Pos. Ctrl (10% FBS)
QTP in 10% FBS
j
SUM159-PT
Migrated cell # /HPF
Neg. ctrl
Pos. ctrl
QTP
k
BT-549
l
m
Treated SUM159-PT
n
Treated BT-549

Figure 5.

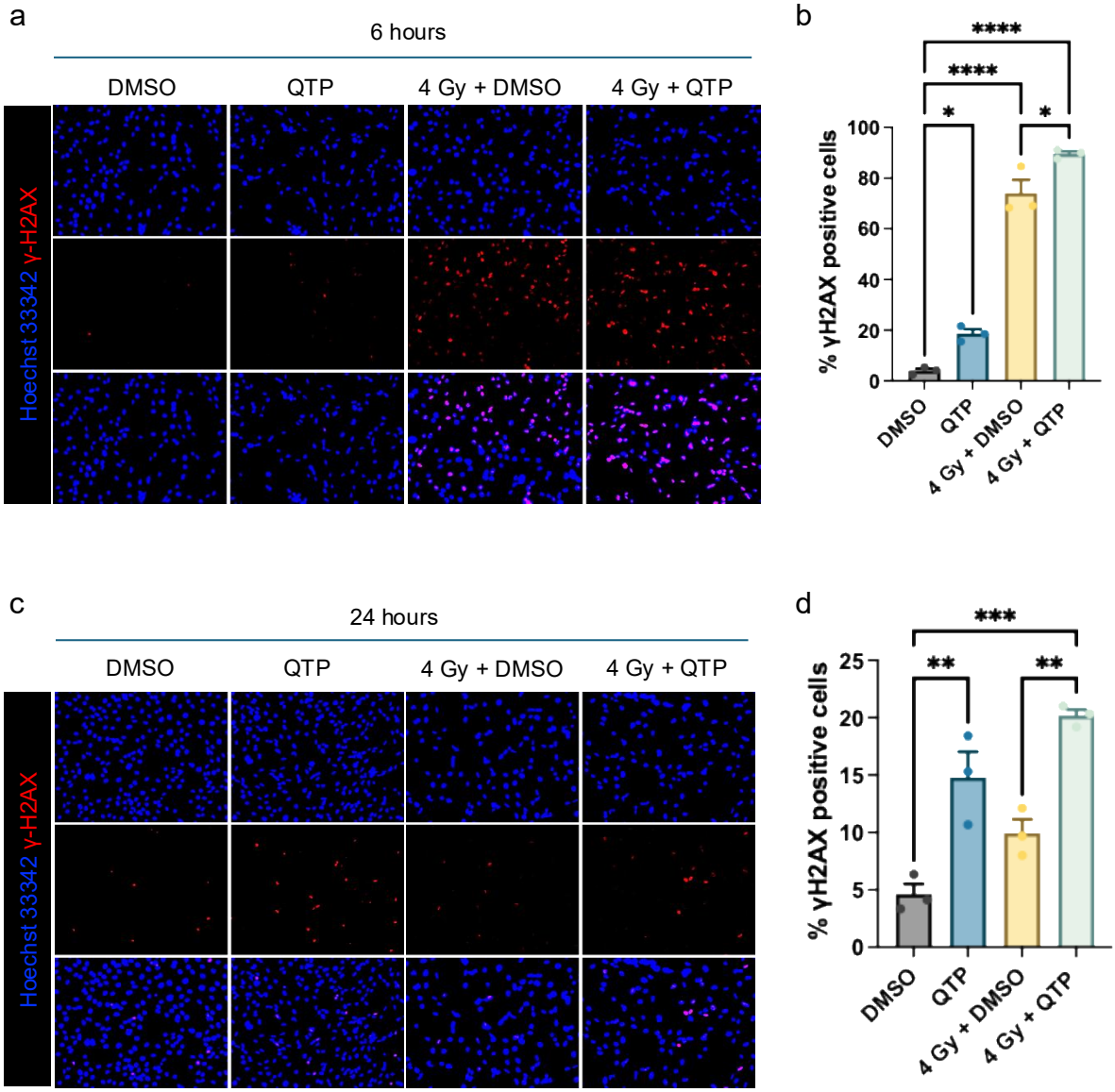
a
6 hours
DMSO
QTP
4 Gy + DMSO
4 Gy + QTP
Hoechst 33342 γ-H2AX
b
% γH2AX positive cells
100
80
60
40
20
0
****
****
*
*
DMSO
QTP
4 Gy + DMSO
4 Gy + QTP
c
24 hours
DMSO
QTP
4 Gy + DMSO
4 Gy + QTP
Hoechst 33342 γ-H2AX
d
% γH2AX positive cells
25
20
15
10
5
0
***
**
**
DMSO
QTP
4 Gy + DMSO
4 Gy + QTP

Figure 6.

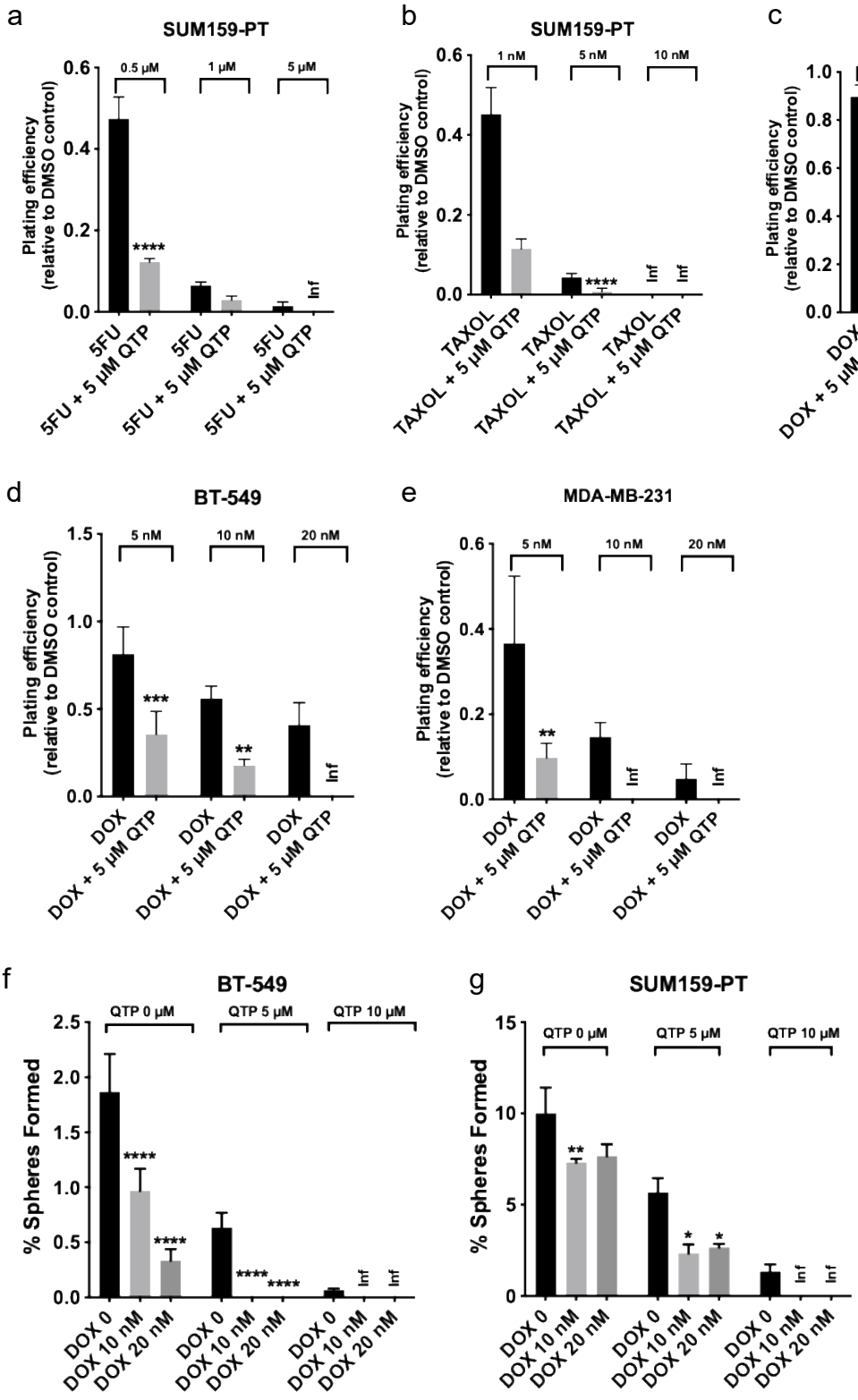
a
SUM159-PT
Plating efficiency (relative to DMSO control)
0.5 μM
1 μM
5 μM
5FU
5FU + 5 μM QTP
****
Inf
b
SUM159-PT
1 nM
5 nM
10 nM
TAXOL
TAXOL + 5 μM QTP
c
SUM159-PT
5 nM
10 nM
20 nM
DOX
DOX + 5 μM QTP
d
BT-549
e
MDA-MB-231
***
**
f
BT-549
QTP 0 μM
QTP 5 μM
QTP 10 μM
% Spheres Formed
DOX 0
DOX 10 nM
DOX 20 nM
g
SUM159-PT
*